

## Supporting Information

### Materials:

$\text{FeCl}_3 \cdot 6\text{H}_2\text{O}$ ,  $\text{CoCl}_2 \cdot 6\text{H}_2\text{O}$ , crystal violet, terephthalic acid, methyl thiazolyl tetrazolium (MTT), Fluorescein diacetate (FDA), Pyridine iodide (PI) and KOH were purchased from Aladdin.  $\text{Bi}(\text{NO}_3)_3 \cdot 5\text{H}_2\text{O}$ ,  $\text{Fe}(\text{NO}_3)_3 \cdot 9\text{H}_2\text{O}$  and trypsin were obtained from Macklin. Ethanol,  $\text{H}_2\text{O}_2$ , NaCl, and ethylene glycol were obtained from BeiJing Chemical Works. Hexadecyltrimethylammonium bromide (CTAB) and 2',7'-dichlorofluorescein diacetate (DCFH-DA) were purchased from Sigma-Aldrich. Agar was purchased from Gentihold. Dulbecco's modified eagle medium was obtained from Gibco. Fetal bovine serum was purchased from Kang Yuan biology. Yeast extract, trypsin soy broth and tryptone were obtained from Thermo Fisher Scientific. *E. coli* (ATCC 25922) and *S. aureus* (ATCC 25923) bacterial strains were obtained from Chuanxiang Biotechnology, Ltd. (Shanghai, China). Ti rods were obtained from Haiyuan Aluminum Special Alloy Co., Ltd. Ultrapure water (18.2 M $\Omega$ ; Millipore Co., USA) was used to prepare all buffers and used in all experiments.

### Synthesis of CFO@BFO nanoceels

$\text{CoFe}_2\text{O}_4$  (CFO) nanoparticles were fabricated by a hydrothermal synthesis approach. For the fabrication of CFO, 0.05 M hexadecyltrimethylammonium bromide (CTAB), 0.1 M  $\text{FeCl}_3 \cdot 6\text{H}_2\text{O}$  and 0.05 M  $\text{CoCl}_2 \cdot 6\text{H}_2\text{O}$  were dissolved in ultrapure water under continuous mechanical stirring. Next, a KOH solution (5.0 M) was added to adjust pH to 11 under vigorous ultrasound for 15 min. Finally, the above solution was transferred to a sealed, Teflon-lined steel autoclave and heated at 180 °C for 12 h.

The obtained black powder was washed with ultrapure water and ethanol and dried overnight at 80 °C.

Next, a precursor of BiFeO<sub>3</sub> (BFO) was prepared by dissolving 160 mg Bi(NO<sub>3</sub>) · 5H<sub>2</sub>O and 121 mg Fe(NO<sub>3</sub>) · 9H<sub>2</sub>O in ethylene glycol. CoFe<sub>2</sub>O<sub>4</sub>@BiFeO<sub>3</sub> core-shell nanostructures were prepared by dispersing 0.05 g of dried CFO nanoparticles into 30 mL of the BFO precursor solution and sonicated for 2 h. This solution was then dried at 80 °C overnight, followed by annealing the dried powder at 600 °C for 2 h at a heating ramp rate of 10 °C min<sup>-1</sup>.

### **The Catalase-Like Activity of nanoeels**

The catalase-like activity of CFO@BFO was assayed by observing the generation of oxygen through the catalytic decomposition of hydrogen peroxide. Firstly, The tubes containing (1) Control, (2) H<sub>2</sub>O<sub>2</sub> (100 μM), (3) Nanoeel (100 μg/mL) and (4) Nanoeel (100 μg/mL) + H<sub>2</sub>O<sub>2</sub> (100 μM), respectively, were reacted for 30 min, and the concentration of dissolved O<sub>2</sub> was measured in real time. Then, the detailed concentrations of H<sub>2</sub>O<sub>2</sub> in different reaction conditions were studied. The calibration curve of absorbance and the concentration of H<sub>2</sub>O<sub>2</sub> (0-8 mM) were recorded by monitoring the absorbance at 240 nm with different concentrations of H<sub>2</sub>O<sub>2</sub>. Besides, the H<sub>2</sub>O<sub>2</sub> decomposition experiments were carried out by adding different concentrations of nanoeels (0-100 μg/mL) in PBS solution (10 mM) containing H<sub>2</sub>O<sub>2</sub> (10 mM) at 37 °C. After a period of time, the mixtures were centrifuged, and the UV-vis spectra of the remaining H<sub>2</sub>O<sub>2</sub> was recorded.

### **ROS Generation Ability**

To quantify the ROS generation efficiency, briefly, nanoeels (100  $\mu\text{g/mL}$ ) were mixed with the solution of DCFH (final concentration of 10  $\mu\text{M}$ ), respectively. Then, the mixture was activated with an alternating magnetic field for different times. The fluorescence intensities under 488 nm excitation ( $\lambda_{\text{ex}}$  of DCF) were detected to determine the ROS generation efficiency.

Then, the  $\bullet\text{OH}$  was determined by the terephthalic acid (TA). TA has negligible fluorescence by itself but is capable of capturing  $\bullet\text{OH}$  and generating 2-hydroxy terephthalic acid with unique fluorescence around 435 nm.

### **Planktonic Bacterial Culture and Antibacterial Experiments**

Monocolony of Escherichia. Coli (*E. coli*) or staphylococcus aureus (*S. aureus*) on the Luria-Bertani (LB) agar plate were transferred to LB culture medium (20 mL) and grew at 37°C for 12 h. Then, the bacteria were diluted to  $10^6$  CFU/mL. The 500  $\mu\text{L}$  of obtained solution was treated with the as-obtained materials at different concentrations with and without magnetic field activated for 30 min. Then the viabilities of bacteria were determined by measuring the optical density at 600 nm after incubating for 8 h.

For solid medium culture, the bacteria solution was diluted  $10^{-4}$  times after irradiation. 100  $\mu\text{L}$  of diluted bacterial solution was streaked on the tryptone agar plates by spread plate method. The plates were cultured at 37 °C for 12 h and the number of colony forming units (CFUs) was counted.

### **Culturing Biofilm**

Monocolony of *S. aureus* strain was incubated in LB culture medium for about 12 h at

37 °C until the OD<sub>600nm</sub> reached 1.0. Then 10 µL of bacteria solution and 990 µL tryptone soy broth (TSB) medium were added into the 24-well plates and incubated at 37 °C without shaking for 48 h. The medium was discarded and freshly added every 24 h, and the biofilms attached on the bottom of wells could be observed after 48 h.

### **In Vitro Bacterial Biofilms Eradication**

The obtained biofilm was mixed with (a) PBS, (b) H<sub>2</sub>O<sub>2</sub> (c) Nanoeels, (d) Nanoeels+H<sub>2</sub>O<sub>2</sub>, (e) PBS+M, (f) H<sub>2</sub>O<sub>2</sub>+M, (g) Nanoeels+M and (h) Nanoeels+H<sub>2</sub>O<sub>2</sub>+M, respectively. H<sub>2</sub>O<sub>2</sub> (100 µM), nanoeels (100 µg/mL). An alternating magnetic field was employed to eradicate the biofilms. After 30 min irradiation, the medium was removed and the remaining biofilm was washed with 1 mL PBS (10 mM).

The remaining biofilms were quantified and observed by Crystal Violet (CV) staining. Briefly, 1 mL of CV (0.2 %) dye was added into the remaining biofilm and incubated at room temperature for 30 min. Then the medium was removed and the biofilms were washed with PBS. To quantify the amount of remaining biofilms, 0.5 mL of 95 % ethanol was added to each well and the optical density at 590 nm (OD<sub>590nm</sub>) was measured.

The condition of bacteria in biofilms was studied by live/dead staining analysis. The biofilms were washed twice with PBS and sequentially stained by FDA (20 µg/mL) and PI (0.5 %) in the dark for 10 min and 30 min, respectively. Then the biofilms were washed three times with PBS and observed by fluorescence microscopy. To study the changes of bacterial morphology, the biofilms were fixed by 4 % formalin

for 15 min and dehydrated with 30 %, 50 %, 70 %, 85 % and 95 % ethanol in turn.

Afterwards, the bacteria were observed using SEM.

### **Cytotoxicity Assays**

After growing in 96-well plates for 24 h, the 3T3 cells were incubated with different concentrations of nanoeels for another 24 h. 20  $\mu$ L of MTT solution (5 mg/mL in PBS) was added to each well and further incubated at 37 °C for 4 h. Then the supernatant was removed and 150  $\mu$ L of dimethyl sulfoxide was added. The cell viability was determined by measuring the absorbance at 490 nm after several times shaking.

### **Hemolysis test of CFO @BFO nanoeels**

1 mL whole blood was collected in tubes containing Li-heparin from the Orbital venous of Kunming mice. Then, 1 mL blood was mixed with 10 mL of PBS (10 mM), centrifuge 5 min at 2500 rpm and remove the supernatant, and repeated 3-4 times until the supernatant became colorless transparent. The precipitated erythrocytes were then dispersed in 1 $\times$ PBS to get erythrocyte suspension. The CFO@BFO nanoeels were added to the erythrocyte suspension to a final concentration of 20, 40, 60, 80, 100  $\mu$ g mL<sup>-1</sup>. Negative control was placed with erythrocyte suspension diluted with 1 $\times$ PBS, Positive control was placed with erythrocyte suspension diluted with ultrapure water. The tubes were incubated for 8 h at room temperature, observe and record the hemolysis phenomenon. At the meanwhile, the specific 540 nm spectrophotometric absorptions of hemoglobin were analyzed. Calculation the hemolysis rate (HR %) by the following equation:

$$\text{HR}\% = (A_{\text{nanoeels}} - A_{\text{NC}}) \times 100\% / (A_{\text{PC}} - A_{\text{NC}})$$

Where  $A_{\text{nanoeels}}$ ,  $A_{\text{PC}}$  and  $A_{\text{NC}}$  are the absorbance of the sample, the positive control and the negative control, respectively.

Subsequently, Kunming mice (n=3) were divided into 3 groups at random, containing PBS (control), nanoeels (7 days and 28 days post injection, 10 mg/kg i.v). After 7 and 28 days, the mice were sacrificed and the blood was used to carry out serum biochemistry assay and complete blood panel analysis at the Changchun Chain Medical Laboratories, Inc. The major organs containing kidney, lung, liver, spleen and heart were collected to stain with H&E.

#### **In vivo biofilm model of an *S. aureus* adhered catheter in mice**

Kunming mice were purchased from the Medical Experimental Animal Center of Jilin University (Changchun, China). The study was performed in strict accordance with the guidelines of Jilin University (Changchun, China) on the Review of Welfare and Ethics of Laboratory Animals and was approved by the Institutional Animal Care and Use Committee (IACUC) of Jilin University (Changchun, China).

To prepare the implants, commercial Ti rods ( $\Phi=2$  mm) were cut into 6 mm segments. Then, biofilm adhered Ti implants were successfully achieved by incubation (37 °C, 48 h) in 1 mL TSB containing  $1 \times 10^5$  CFU of *S.aureus* (n=5). Finally, the implants were rinsed with PBS (pH 7.4) and immediately implanted subcutaneously through a minimal surgical incision in the inner thigh of previously anaesthetized mice. 200  $\mu\text{L}$  of PBS was administrated as the control group. Nanoeels (1 mg  $\text{mL}^{-1}$ , 200  $\mu\text{L}$ ) were respectively injected subcutaneously into other groups with different treatments. Then the implanted site was activated by magnetic field at 4 h after the injection.

All mice were euthanatized and the implanted catheters were taken out after 7 days. SEM and histological analysis used to evaluate the biofilm eradication. The tissues were collected (implantation site, heart, liver, kidney, lungs, and spleen) and fixed in neutral buffered formalin (10%). Finally, embedding in paraffin, sectioning (4  $\mu\text{m}$  thick), and staining with H&E were performed for the fixed tissues. The histological sections were observed with an optical microscope.

### **Statistical Analysis**

All data were expressed in this article as mean result  $\pm$  standard deviation (SD). All results were obtained from several independent experiments with similar results. Statistical evaluation was performed using analysis of variance (Student's test).

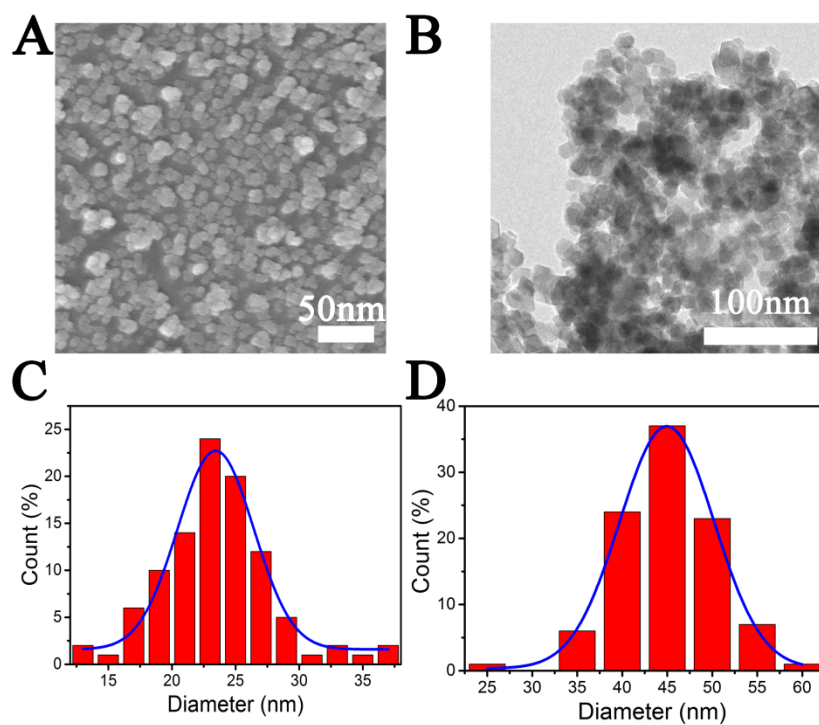


Figure S1. A) Scanning electron microscopy (SEM) image of CFO. B) Transmission electron microscopy (TEM) image of CFO@BFO. C) Size distribution of CFO. D) Size distribution of CFO@BFO nanoecels.



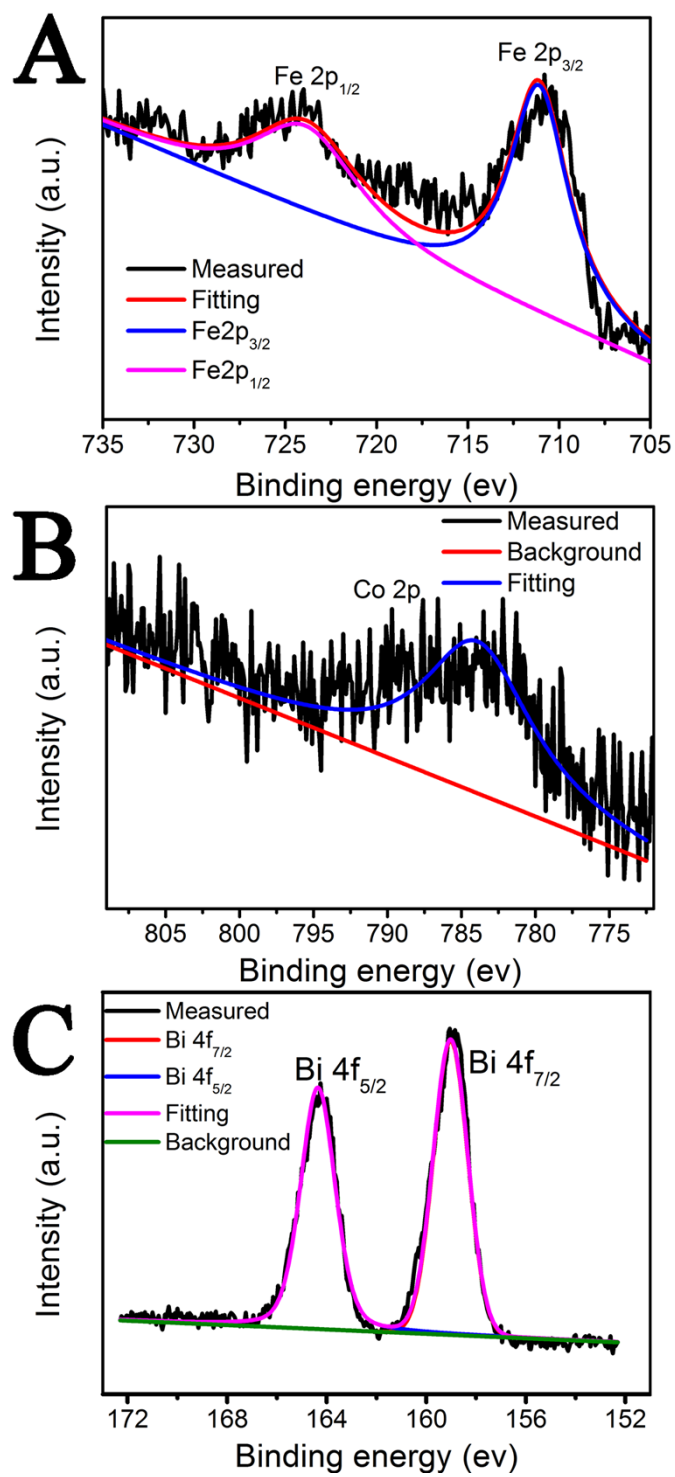


Figure S2. X-ray photoelectron spectroscopy (XPS) of (A) Fe 2p, (B) Co 2p and (C) Bi 4f.

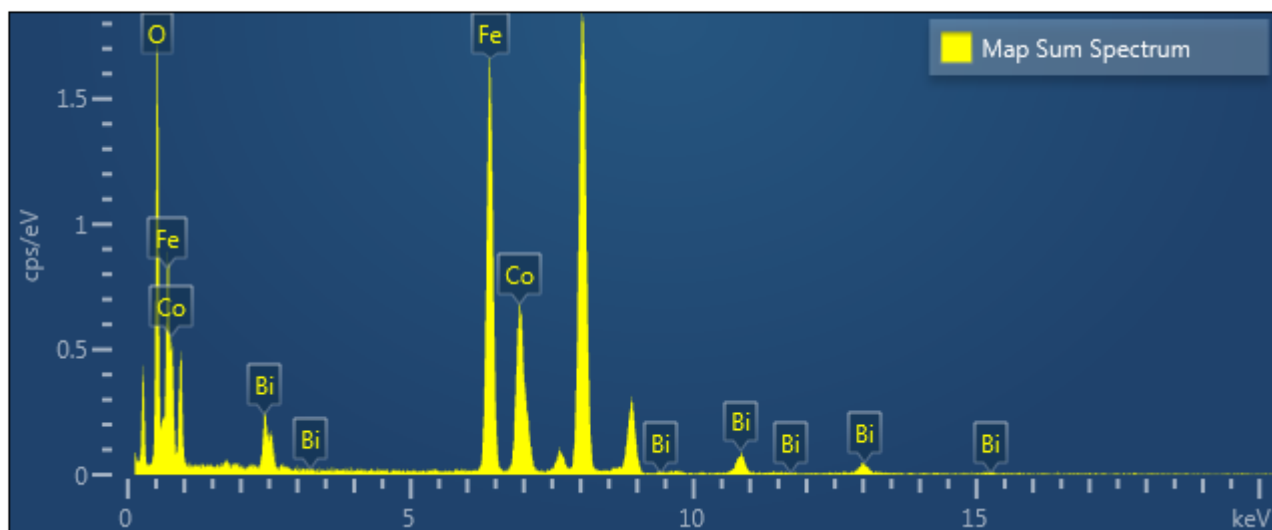


Figure S3. An energy-dispersive spectroscopy (EDS) analysis of nanoceels.

Element	Line Type	k factor	Wt%
O	K series	1.86867	28.00
Fe	K series	1.19079	42.59
Co	K series	1.26119	19.89
Bi	M series	1.73929	9.52
Total:			100.00

Table S1. The content of O, Fe, Co and Bi in CFO@BFO nanoeel.

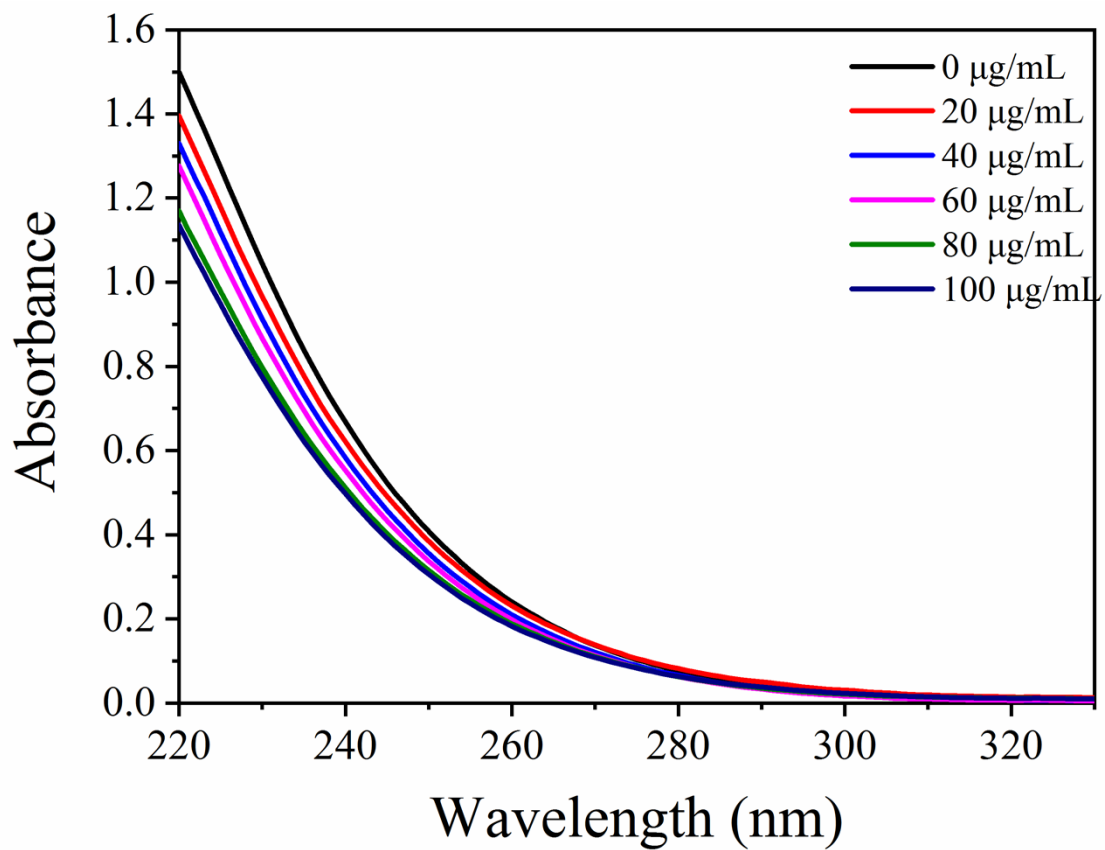


Figure S4. UV-vis spectra of H<sub>2</sub>O<sub>2</sub> were recorded after incubation with different concentration of nanozeolites.

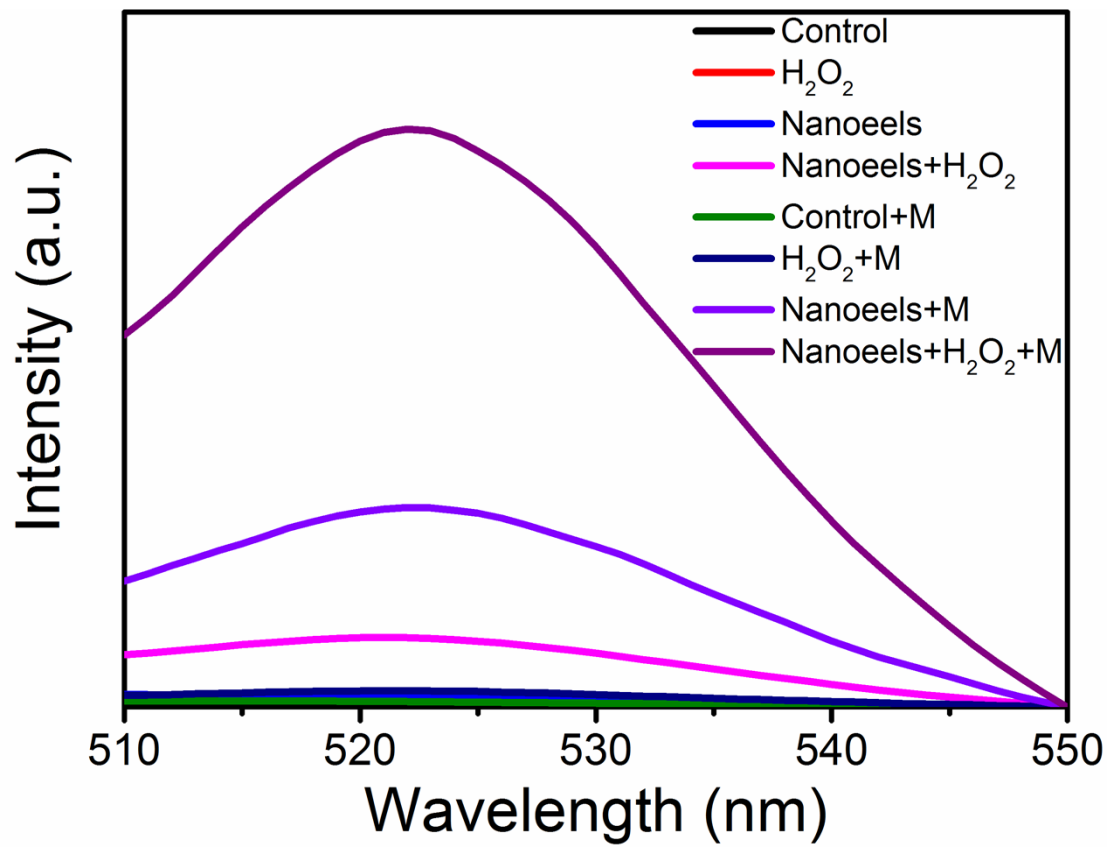


Figure S5. ROS generation ability of nanoeels under AMF activation.

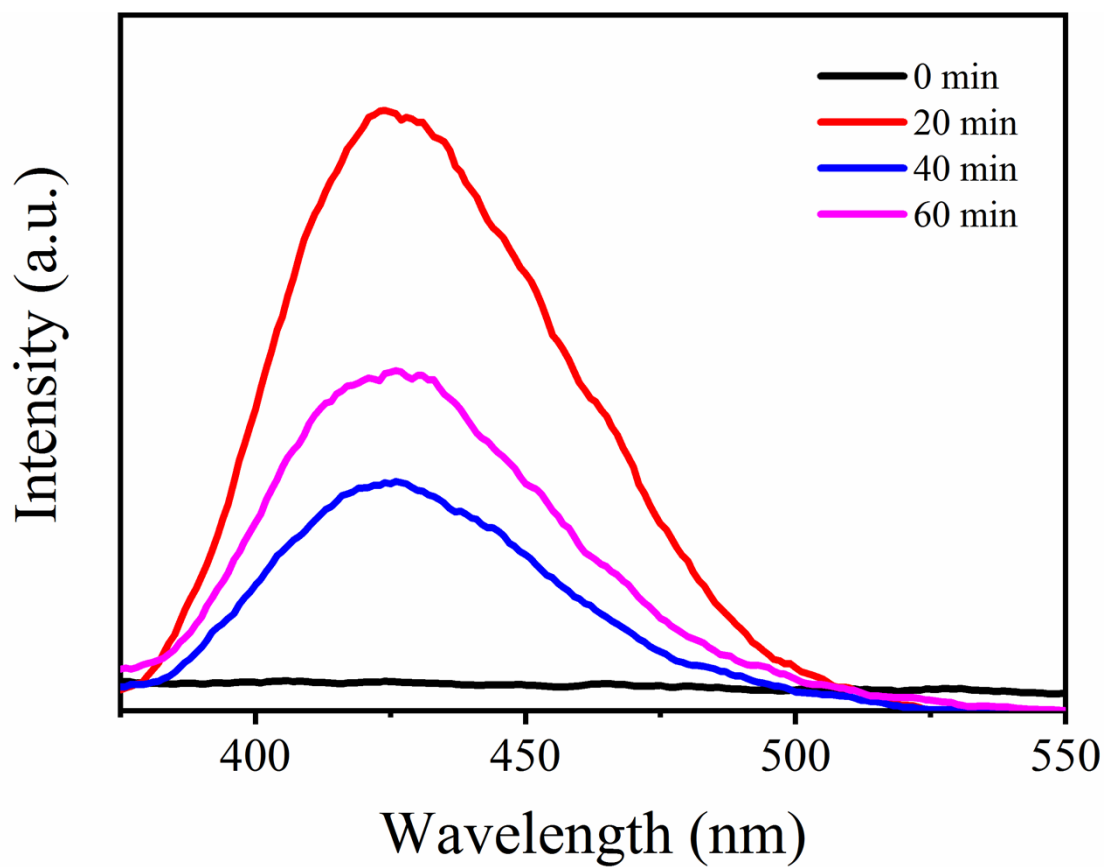


Figure S6. Fluorescence spectra of TA incubated with CFO@BFO nanoels to demonstrate the generation of  $\cdot\text{OH}$ .

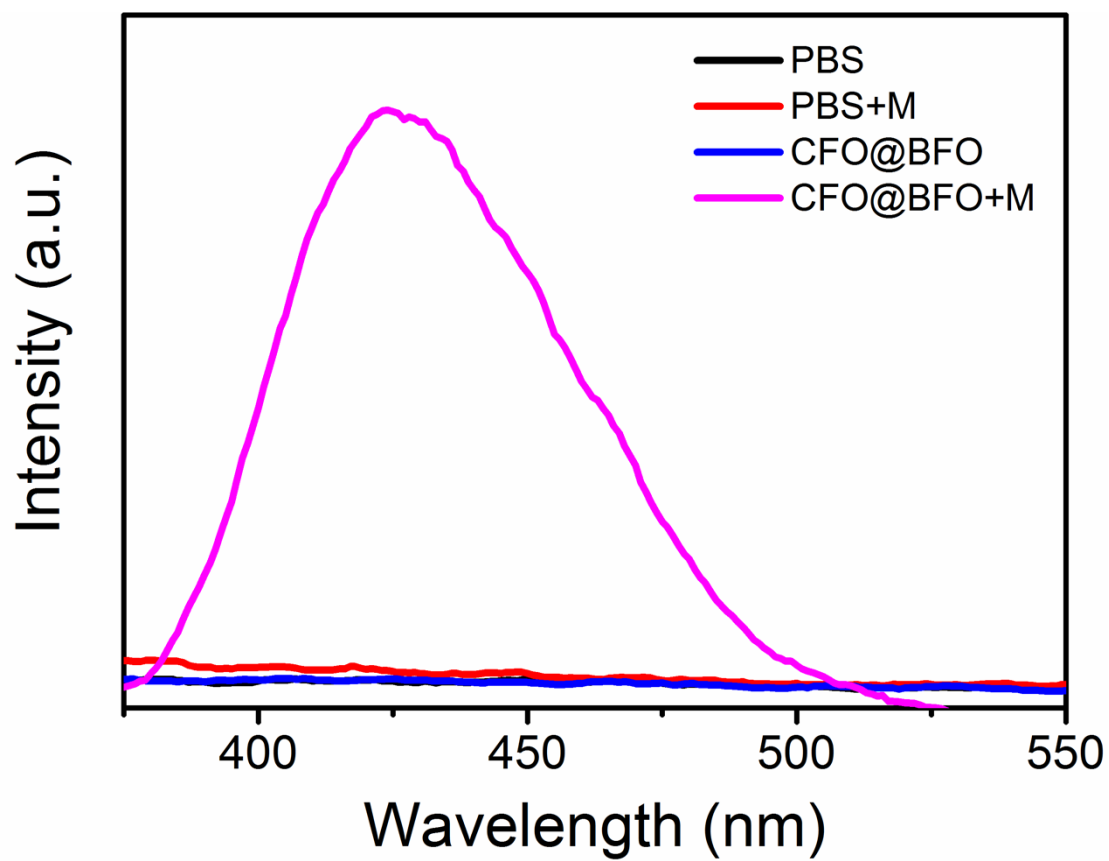


Figure S7. The generation of  $\bullet\text{OH}$  with different treatments.

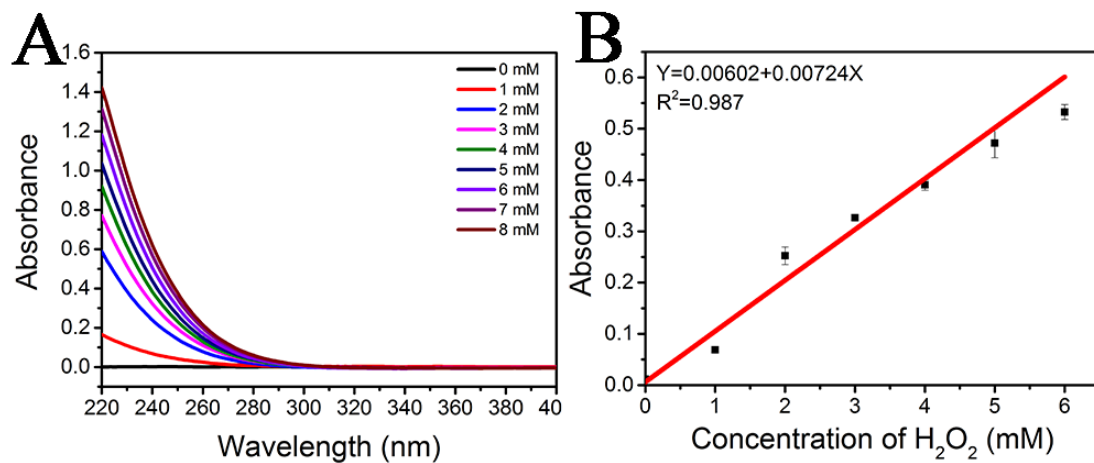


Figure S8. a) The UV-Vis spectra of H<sub>2</sub>O<sub>2</sub> (1-8 mM); b) The calibration curve of absorbance at 240 nm and the concentration of H<sub>2</sub>O<sub>2</sub>.



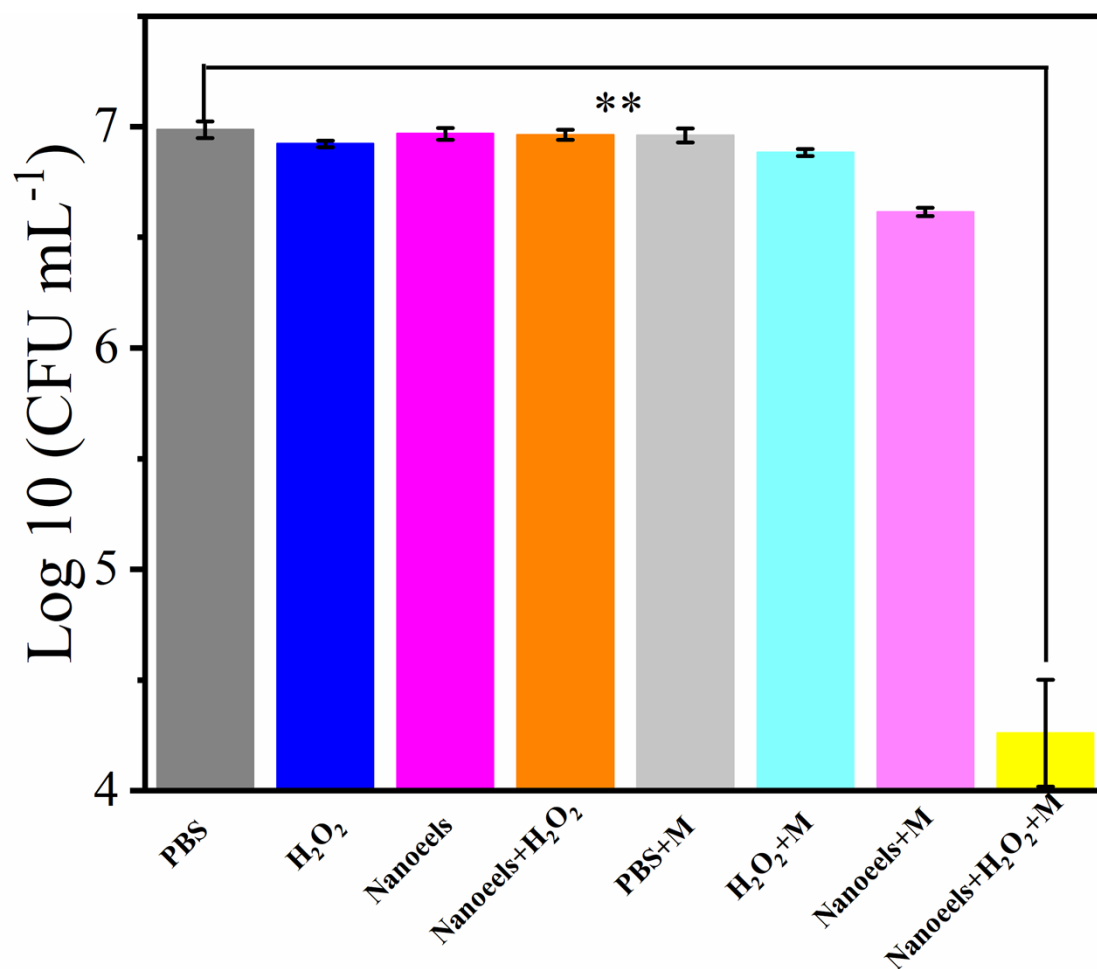


Figure S9. Viability analyses of *E. coli* by different treatments. Data were presented as mean  $\pm$  s.d. (n = 3). Asterisks indicate significantly differences (\*P < 0.05, \*\*P < 0.01, \*\*\*P < 0.001).

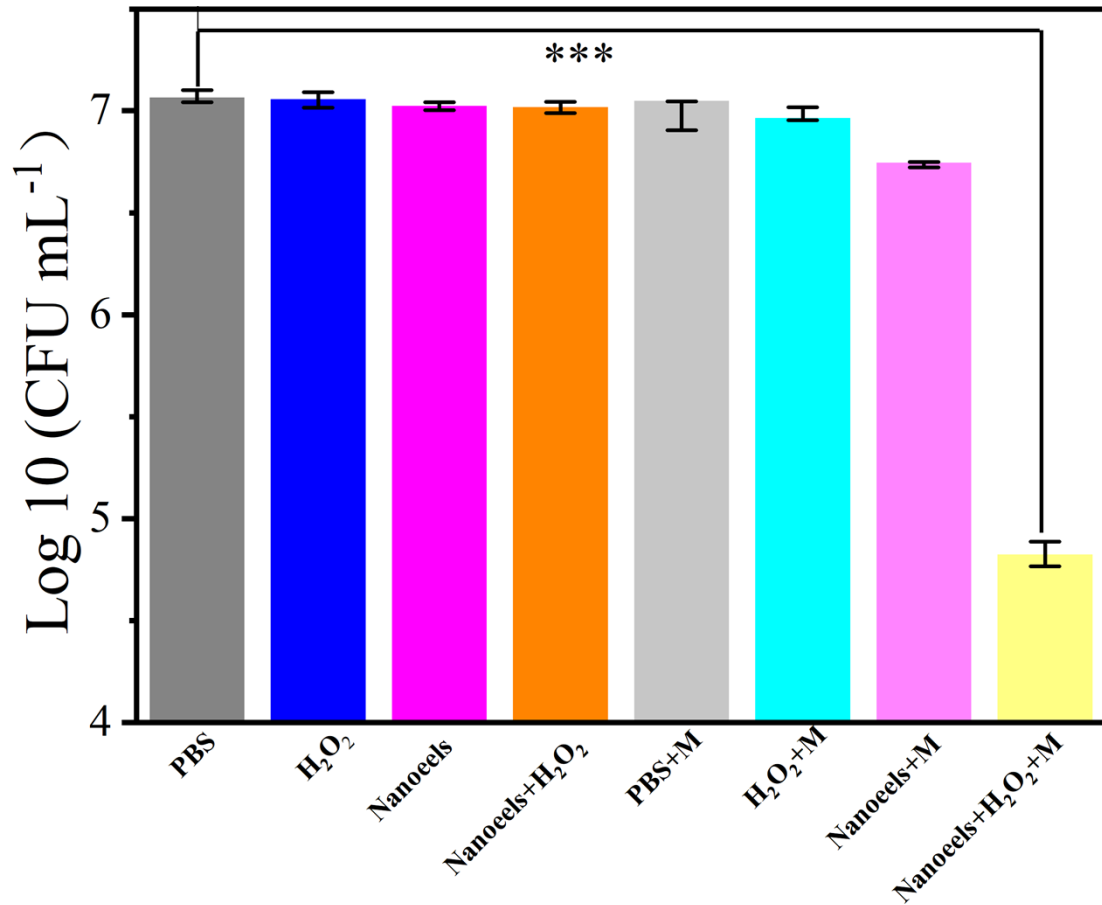


Figure S10. Viability analyses of *S. aureus* by different treatments. Data were presented as mean  $\pm$  s.d. (n = 3). Asterisks indicate significantly differences (\*P < 0.05, \*\*P < 0.01, \*\*\*P < 0.001).

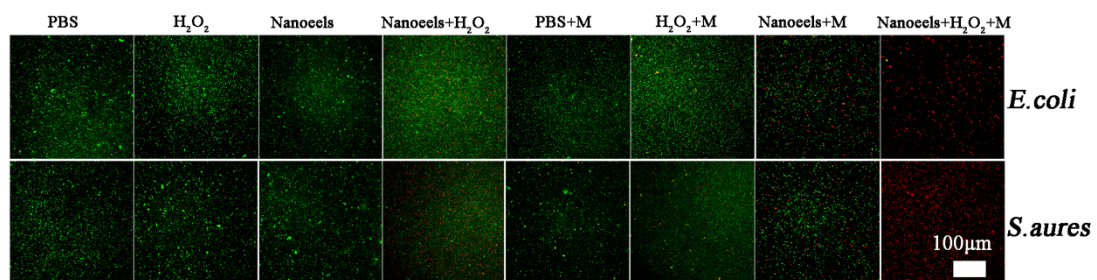


Figure S11. Typical fluorescence images of *E. coli* (top) and *S. aureus* (below) by various treatments.

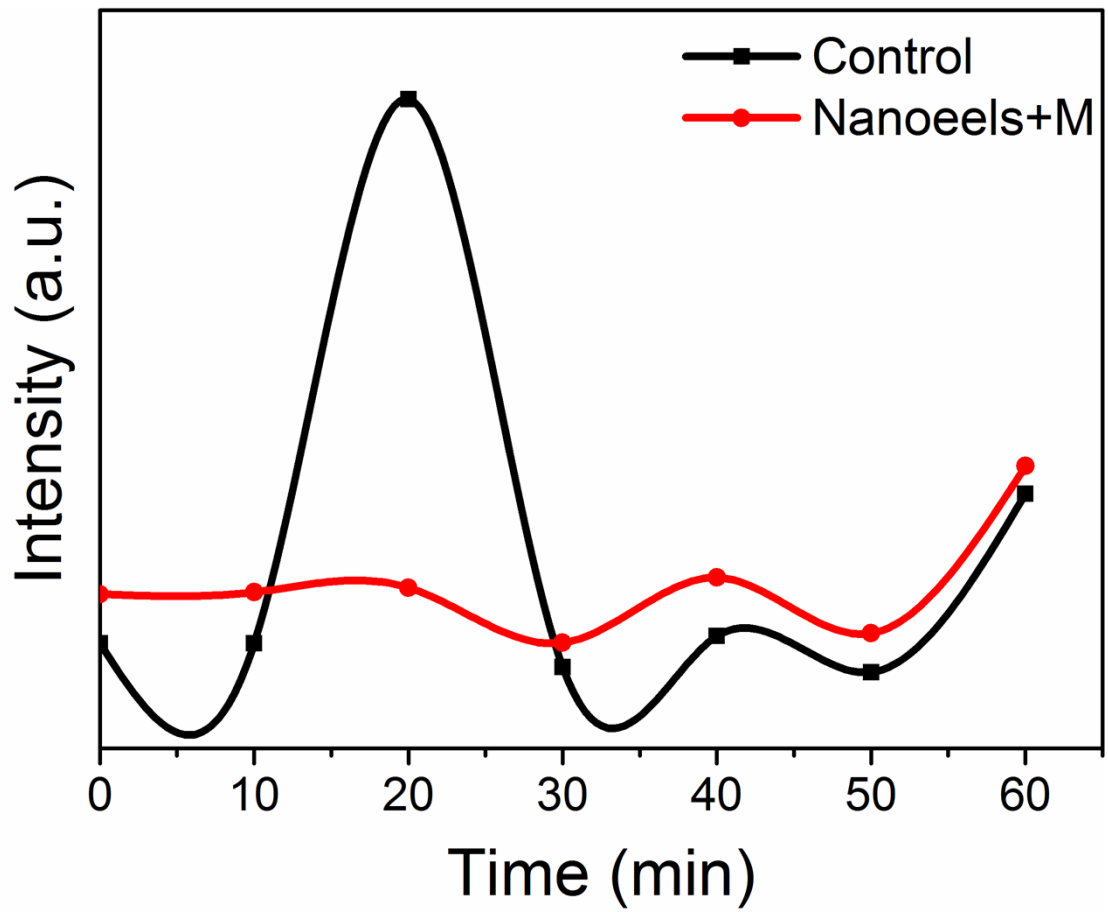


Figure S12. Analysis of the cell membrane potential of *S. aureus* cells treated with nanoeels (100  $\mu\text{g}/\text{mL}$ ). Control: untreated *S. aureus*.

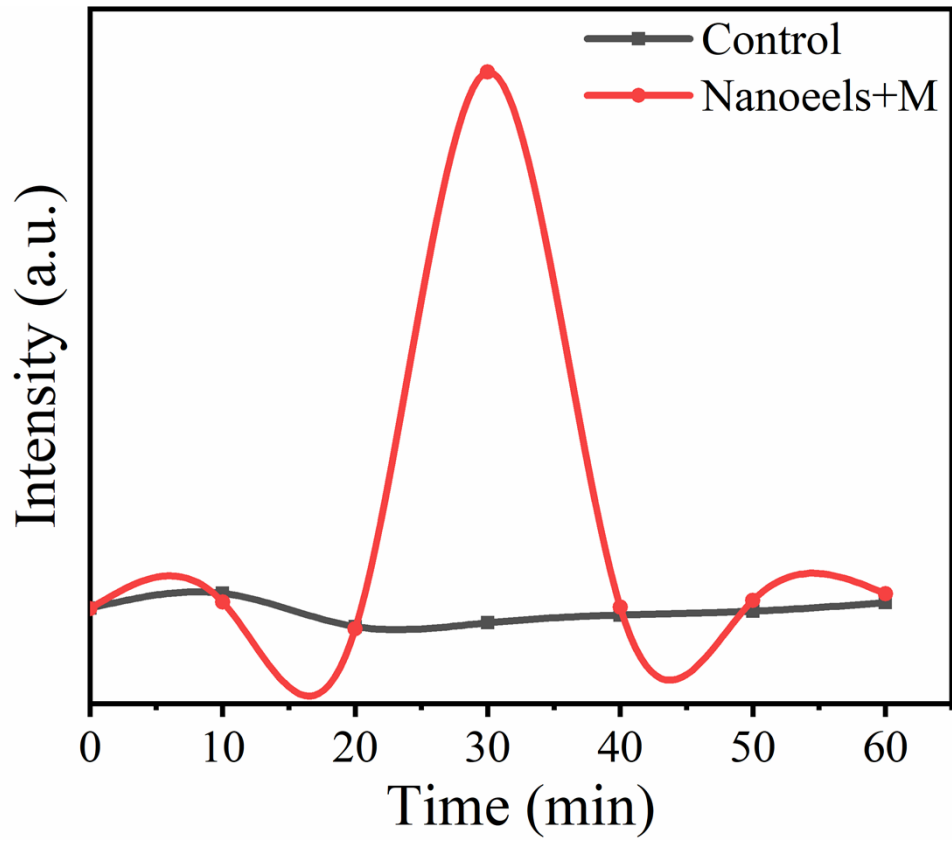


Figure S13. Analysis of the cell membrane potential of *E. coli* cells treated with nanoeels (100  $\mu\text{g}/\text{mL}$ ). Control: untreated *E. coli*.

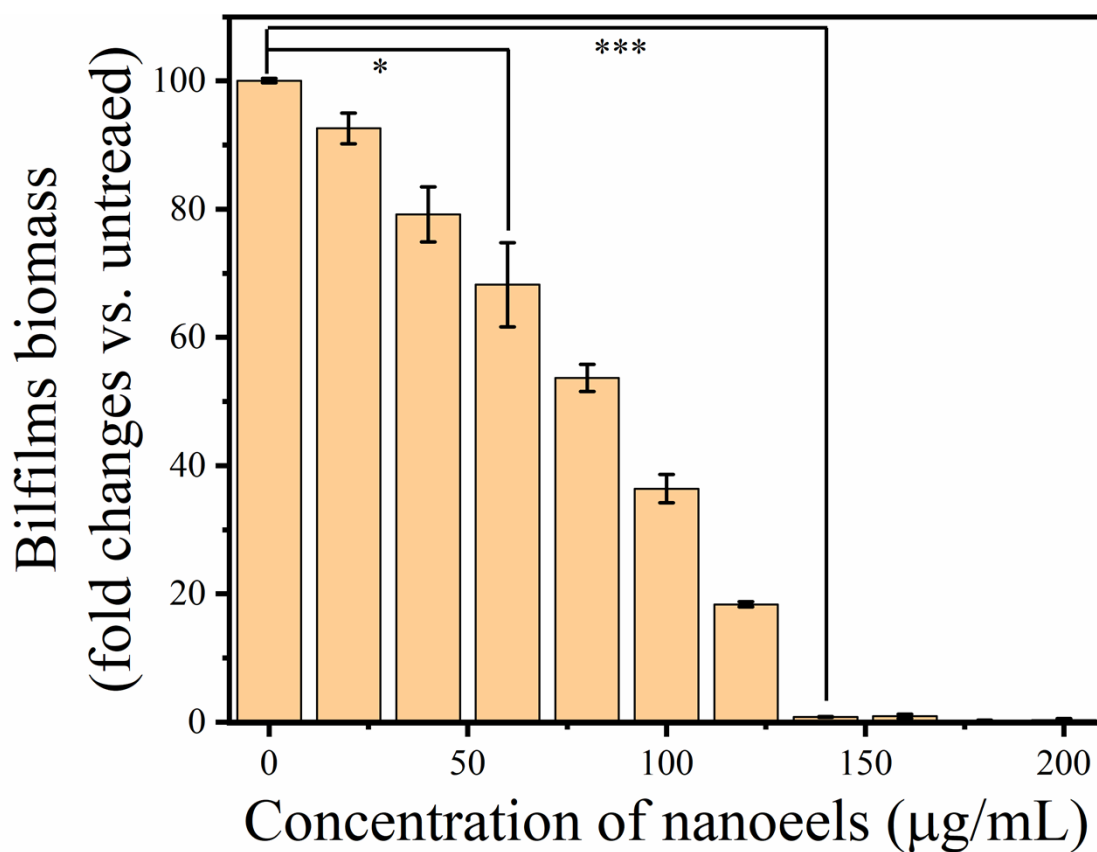


Figure S14 Different concentrations of CFO@BFO nanozeels for inhibition bacteria biofilm growth under magnetic field ( $H_2O_2$ : 100  $\mu$ M). Asterisks indicate significantly differences (\* $P < 0.05$ , \*\* $P < 0.01$ , \*\*\* $P < 0.001$ ).

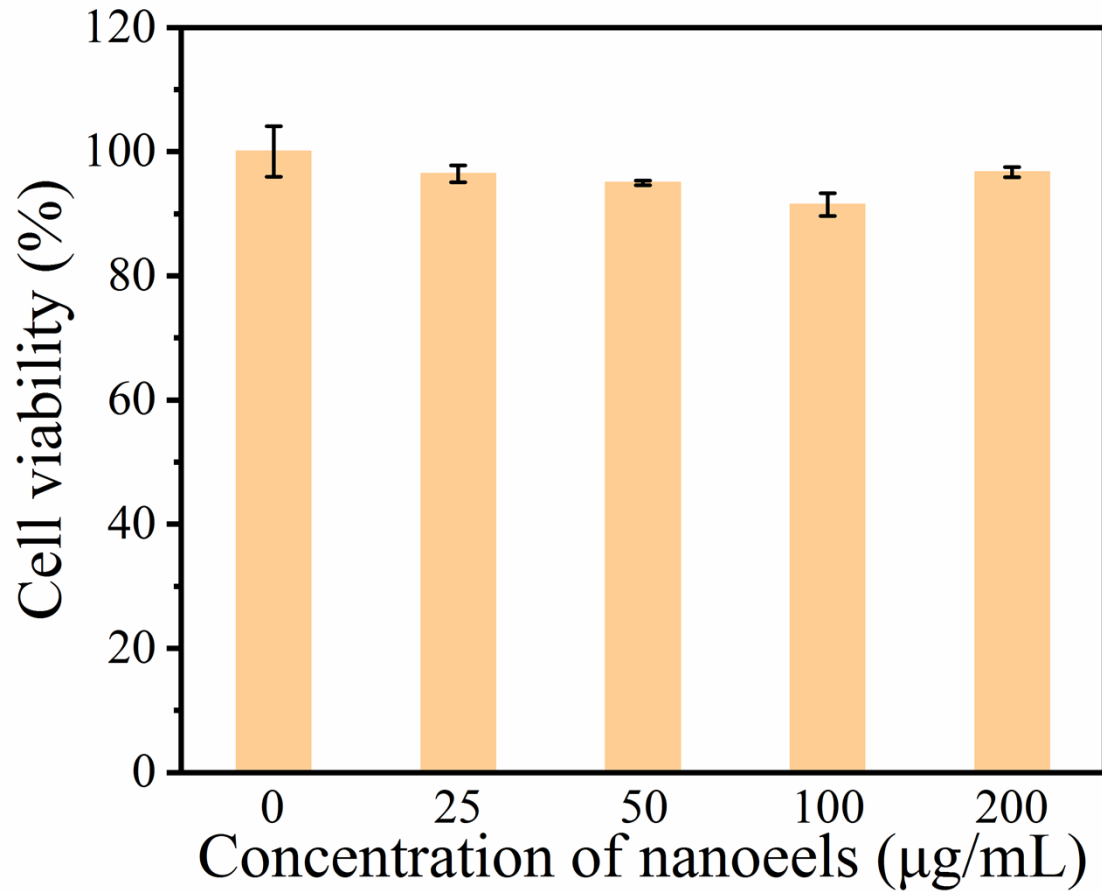


Figure S15. Cytotoxicity studies by MTT assay for RAW cells after incubation with various concentrations of CFO@BFO nanoeeel for 24 h. Data were presented as mean  $\pm$  s.d. (n = 5).

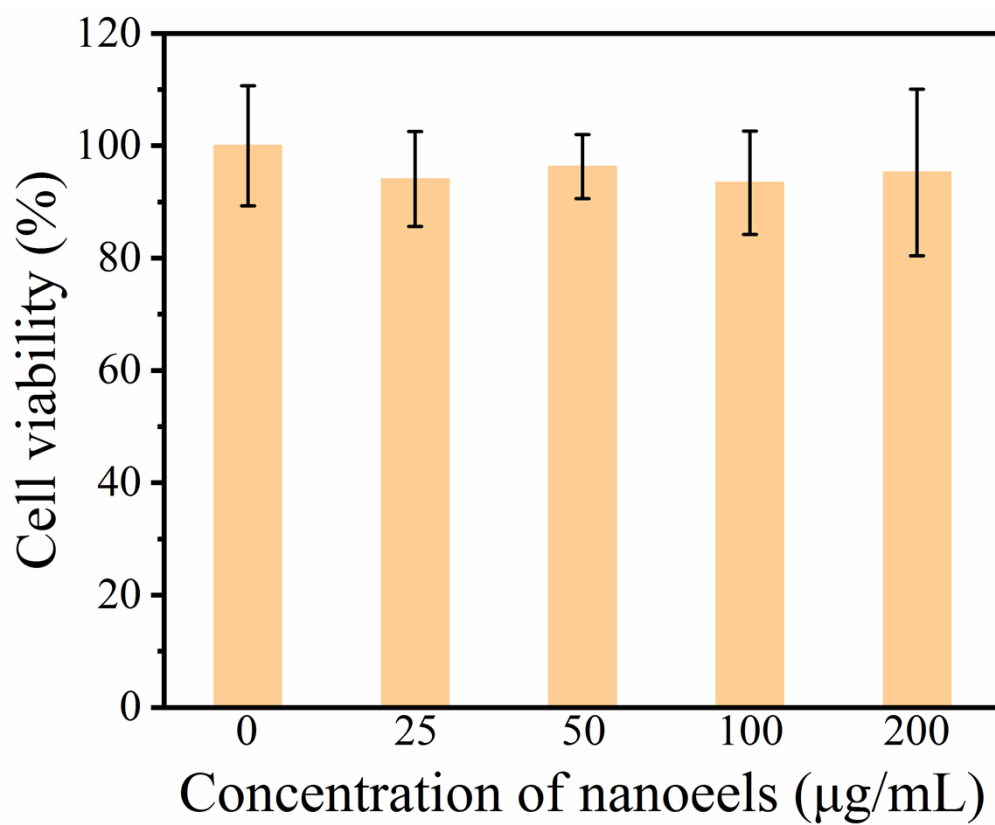


Figure S16. Cytotoxicity studies by MTT assay for 3T3 cells after incubation with various concentrations of CFO@BFO nanoceels for 24 h. Data were presented as mean  $\pm$  s.d. (n = 5).



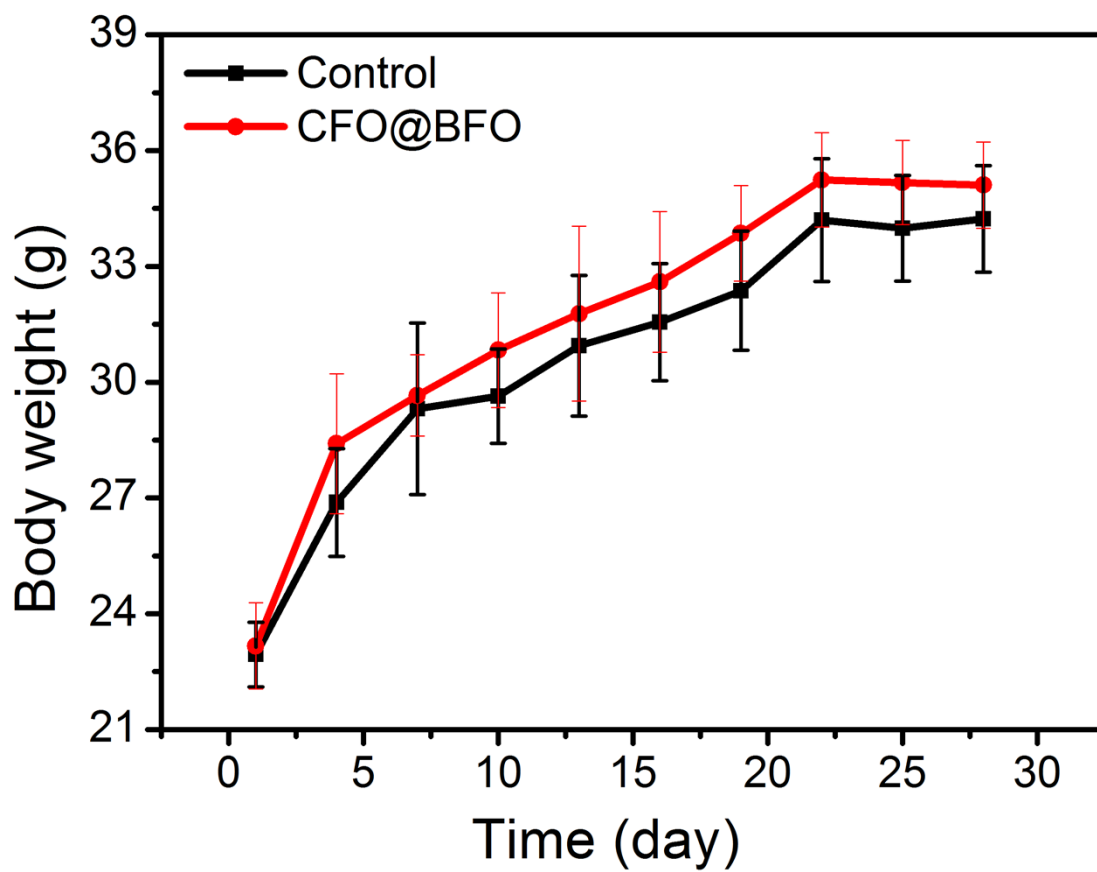


Figure S17. Mice body weight after treated with various groups. Data were presented as mean  $\pm$  s.d. (n = 3).

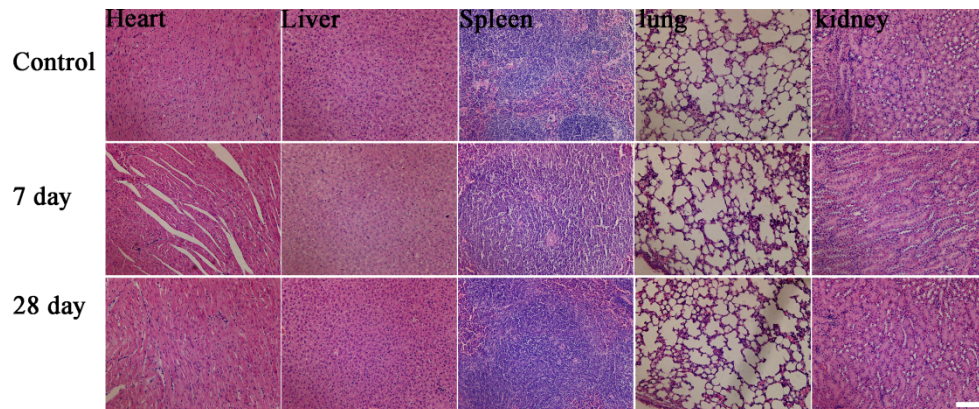


Figure S18. H&E staining assays of the major organs from all experimental groups.

The scale bar was 100  $\mu\text{m}$ .

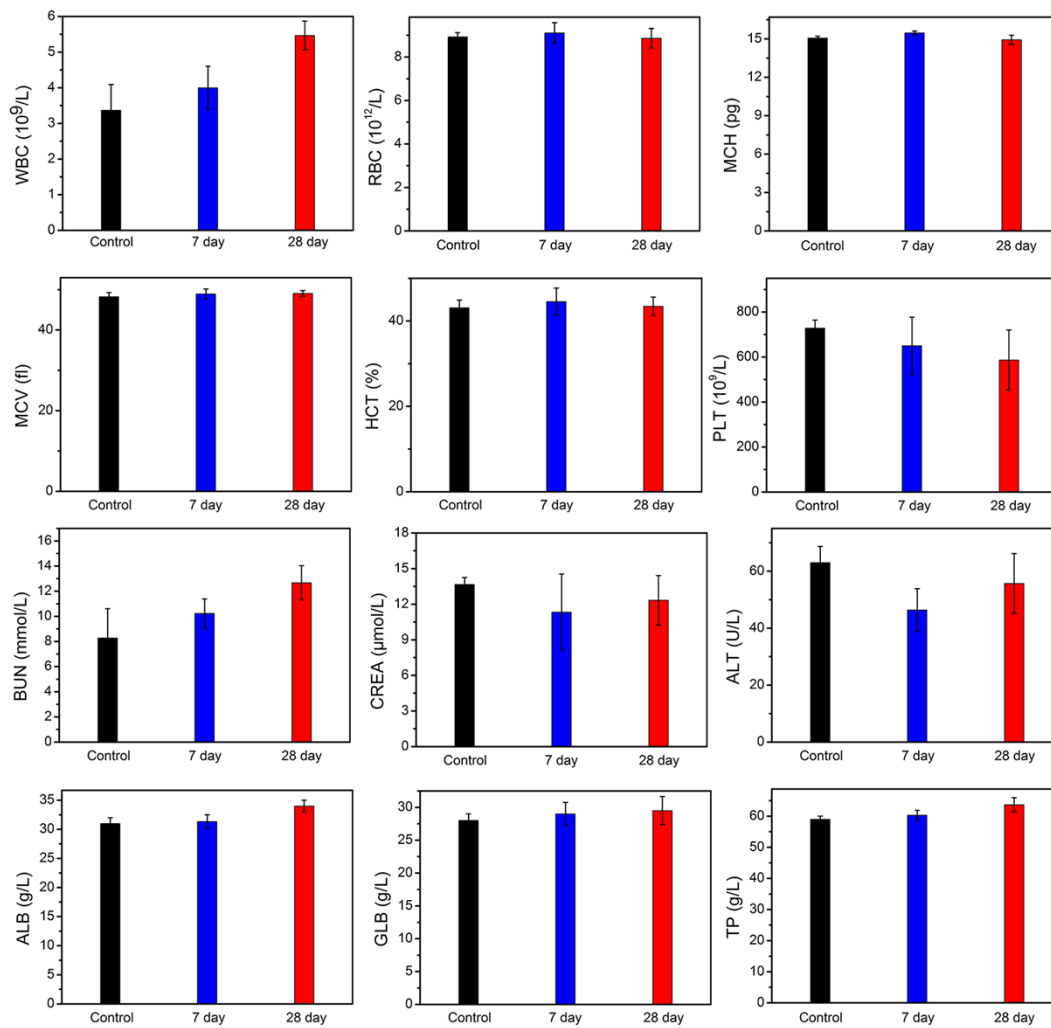


Figure S19. Blood biochemical levels and hematological parameters of the mice after treatment with CFO@BFO nanoels for 7 and 28 days. Data were presented as mean  $\pm$  s.d. (n = 3).

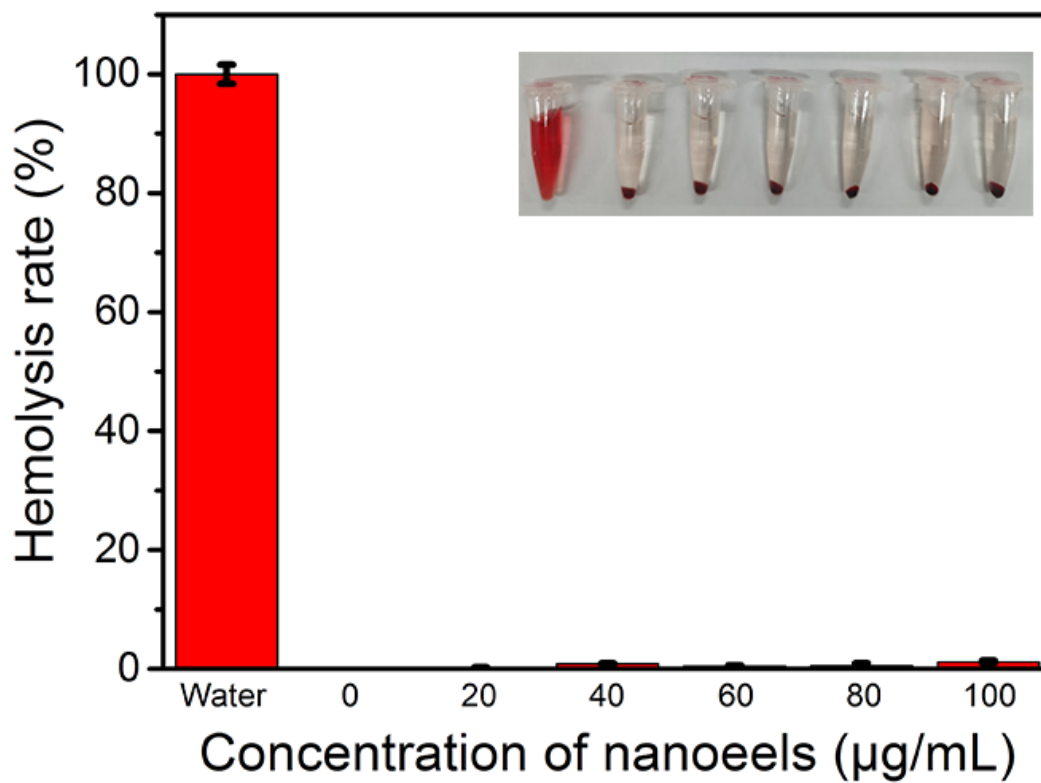


Figure S20. Hemolysis rate (HR%) of nanoeeels. Data were presented as mean  $\pm$  s.d. (n = 3).

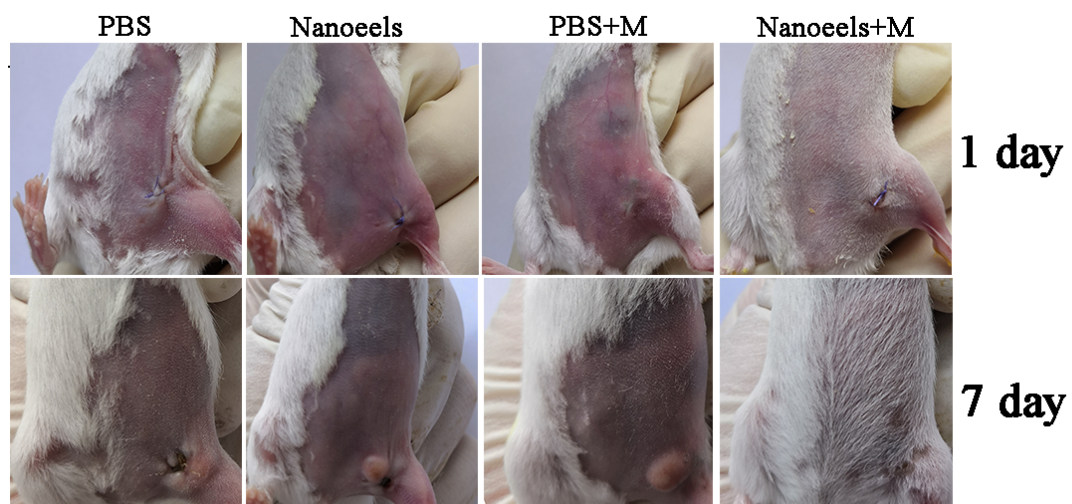


Figure S21. Photos of mice with suffered implant-related bacterial infection from four groups at different times during the therapeutic process.

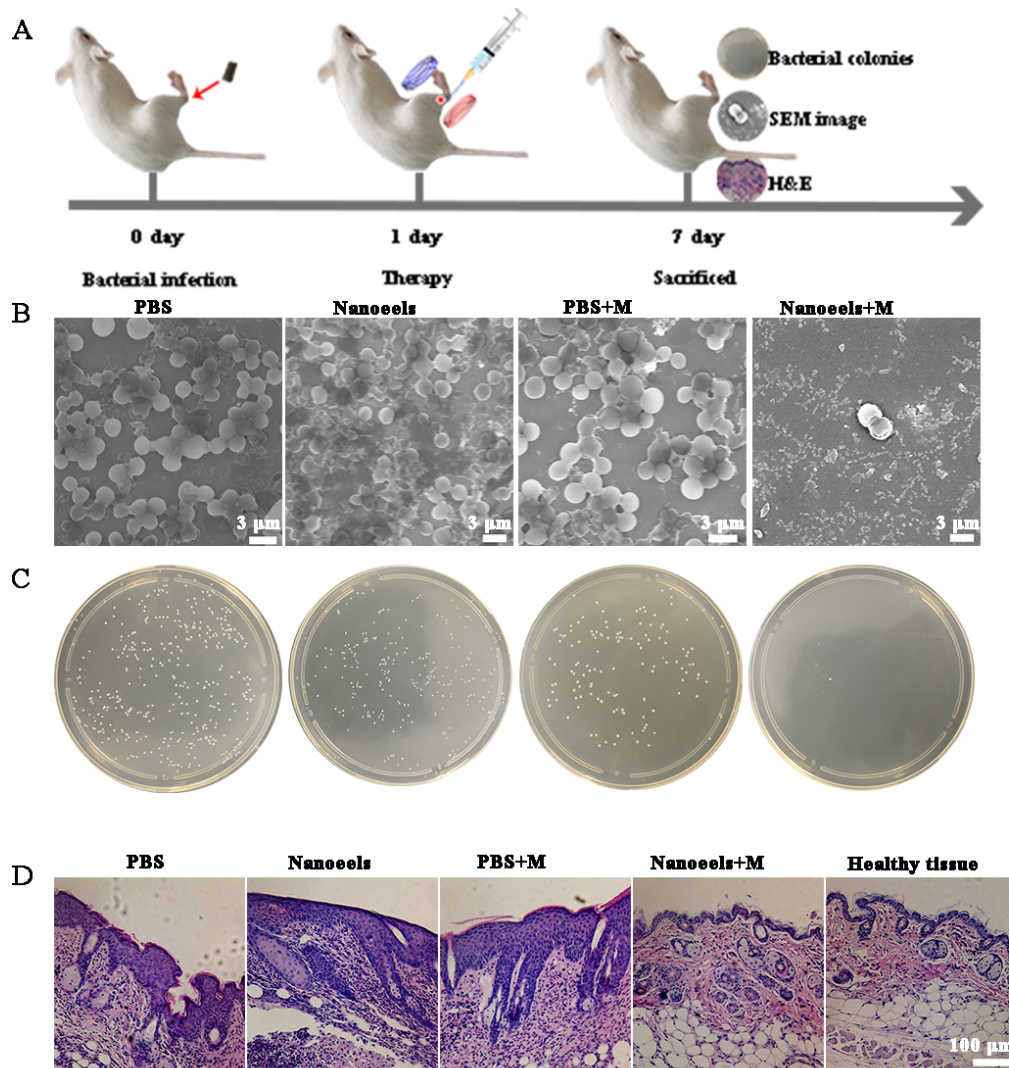


Figure S22. A) Schematic illustration of the treatment strategy for implant-related bacterial infection model. B) SEM photos of implants surfaces after different treatments. C) The bacteria on the surface of the implant were incubated on agar plates. D) H&E analysis of infected skin tissue after different treatments.

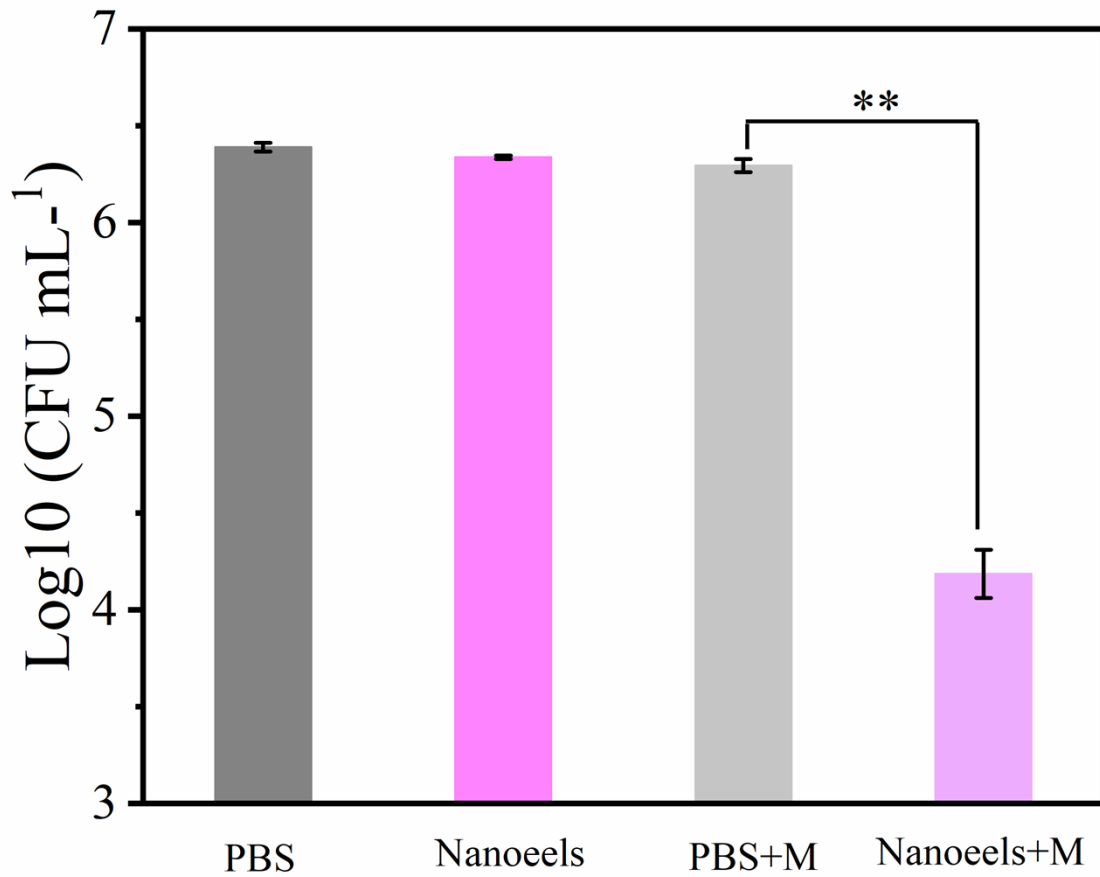


Figure S23. The surviving bacteria in the wound tissue were quantified Data were presented as mean  $\pm$  s.d. (n = 3). Asterisks indicate significantly differences (\*P < 0.05, \*\*P < 0.01, \*\*\*P < 0.001).